X-ray emission by ultrafast inner-shell ionization from vapors of Na, Mg, and Al

Kengo Moribayashi,[1] Akira Sasaki,[1] and T. Tajima[1,2]
[1]*Advanced Photon Research Center, Japan Atomic Energy Research Institute, 25-1, Mii-minami-cho, Neyagawa-shi, Osaka 572-0019, Japan*
[2]*Department of Physics and Institute for Fusion Studies, University of Texas at Austin, Austin, Texas 78712*
(Received 18 August 1998; revised manuscript received 19 October 1998)

The optimization of the physical processes of an inner-shell ionization x-ray laser is carried out theoretically. Vapors of Na, Mg, and Al are adopted as a target material in order to avoid deleterious fast atomic processes except for the inner-shell ionization process. The effects of the vapor density and x-ray intensity are studied. Larmor x rays are suitable as a pump x-ray source because they have high brightness and short pulse. Their peak intensity and energy spectrum are appropriate for inner-shell ionization. In the Mg vapor the gain of 10 and $10^3\,\mathrm{cm}^{-1}$ can be obtained with the use of 10^{11}- and $10^{14}\,\mathrm{W/cm}^2$ intensity x rays, respectively. [S1050-2947(99)00104-3]

PACS number(s): 32.80.Hd, 32.80.−t, 42.55.Vc, 52.25.Nr

I. INTRODUCTION

An x-ray-pumped inner-shell ionization laser has been thought to be among the useful methods for x-ray laser emission [1–10]. Silfvast *et al.* [7] produced the laser at 441.6 and 325 nm of Cd vapor pumped by a 12-eV soft-x-ray source with an approximated, blackbody distribution. Kapteyn and co-workers [8,9] made a laser at 108.9 nm by the inner-shell ionization of Xe atom. However, there has been no experimental demonstration of x-ray laser emission through this process to the best of our knowledge. In order to realize an inner-shell ionization x-ray laser, a higher brightness x-ray pumping source with higher photon energy is needed. (Meyer *et al.* [10] seem to have planned to employ a neonlike germanium soft-x-ray laser as a pump source for an inner-shell ionization x-ray laser in Na vapor.) The necessary brightness and photon energy of x rays are determined by target materials. In this paper we search for advantageous target materials as well as x-ray sources for the purpose of optimizing the physical processes of an inner-shell ionization x-ray laser.

The inner-shell ionization x-ray laser method was first proposed by Duguay and Rentzepis [1]. Kapteyn [3] and Moon, *et al.* [4] theoretically showed that the lasing gain of 10 cm^{-1} associated with the $K\alpha$ transitions is possible by irradiating x rays of $10^{14}\sim10^{15}\,\mathrm{W/cm}^2$ intensity and 50-fs duration on Ne or C atoms. In our previous paper [6] we showed that the key to producing an x-ray laser is the choice of target materials; we compared sodium atoms and carbon atoms. The inner-shell $2p$ electron ionization cross sections of sodium atoms are much greater than those of the $1s$ electrons in carbon atoms. Therefore, the use of sodium atoms reduces the necessary intensity of an x-ray source. We also showed [6] that ultrafast inner-shell ionization processes, much faster than any other atomic processes, lead to a high conversion efficiency. Here we suggest making use of an ultrafast inner-shell ionization process while increasing the lifetime of inner-shell excited states (upper states) and reducing the secondary electron impact ionization rate. Let us note, as shown in Ref. [11], that the inner-shell excited state of a $(2p)^{-1}$ hole in low Z matter such as Na, Mg, and Al atoms has a much slower decay than a K- and L-shell hole of any other atoms. (These materials were also selected in our previous paper [6] because of large inner-shell ionization cross sections.) In order to avoid secondary electron impact ionization effect, Kapteyn [3] and Moon *et al.* [4] required a relatively low density ($10^{20}\,\mathrm{cm}^{-3}$), which unfortunately amounts to a (relatively) low gain. We show that a sufficiently large gain can be obtained if we adopt the Na, Mg, and Al vapors with a density of $10^{17}\sim10^{19}\,\mathrm{cm}^{-3}$. (Meyer *et al.* [10] have also considered Na vapor as a target material.) Our system of choice is an extension of that in the experimental demonstration by Silfvast *et al.* [7], who selected no Auger states for the upper states of laser ($4d^9 5s^2\ ^2D$) and a lower density of $10^{16}\sim10^{17}\,\mathrm{cm}^{-3}$.

A blackbody x-ray source has often been used as a pumping source [3,4,7–9,12]. In addition, the Larmor x-ray source [6] may be employed. A recent progress of intense pulsed lasers gives us new sources of high-brightness short-pulse x rays, such as the Larmor radiation [13] (due to the acceleration of electrons in the laser electromagnetic fields), as well as the high harmonic generation [14], which is based on laser-driven periodic bremsstrahlung. (Note that the Larmor x-ray radiation has been well known, as written in Ref. [13]. It has not yet been observed experimentally; however, the laser intensity just begins to reach an order of $10^{20}\,\mathrm{W/cm}^2$.) Especially we consider the laser-induced Larmor radiation x rays driven by relativistic short laser pulses because their features (which follow) are suitable for a pumping source as is demonstrated in Sec. IV B. (i) The radiative spectrum of Larmor x rays has a peak at $\omega=a_0^3\omega_0$, where ω_0 and a_0 are the laser frequency and normalized laser field ($a_0=eE_0/m\omega_0 c$). This is in contrast to the bremsstrahlung whose spectrum is flat. Only when the laser power enters the relativistic regime ($a_0\geqslant1$), the laser-induced Larmor x rays begin to appear. (ii) The radiative power of the Larmor x ray increases linearly, proportional to the laser intensity and to the density of electrons, whereas the bremsstrahlung power increases in proportion to 1.5 powers of the laser intensity and square of the electron density. The intensity (in $\mathrm{W/cm}^2$) of the Larmor x ray in the linear regime is [15,16]

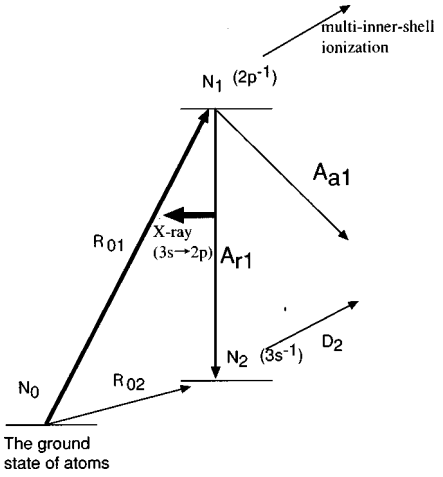

FIG. 1. Atomic processes in x-ray emission from the singly excited states.

$$L_{\mathrm{LX}} \sim 10^{11} a_0^2 \frac{a_0^2+8}{2a_0^2+8} (10^{-21} n_e) \times (R_s)^2 \frac{1}{(1+4\pi R_s/\lambda_L a_0^2)(1+2\pi R_s/\lambda_L a_0)}, \quad (1)$$

where n_e, λ_L, and R_s are the electron density (units of cm^{-3}), wavelength (units of μm) of the laser, and diameter (units of μm) of spot size. For example, at the laser power of 30 TW focused on a target (electron density $n_e = 3 \times 10^{22}\,\mathrm{cm}^{-3}$) with $R_s = 5\ \mu$m ($a_0 = 5$, $\lambda_L = 0.88$), the x-ray intensity due to the Larmor radiation is $\sim 10^{14}$ W/cm^2 and the peak energy is about 100 eV ($\sim 10^{11}$ W/cm^2 for the blackbody x rays with the same peak energy according to Stefan-Boltzmann's law of radiation). Since the large population of the upper states (inner-shell excited states) is required to obtain high gain, high brightness x rays are important to overcome the loss of population due to the fast Auger process. (iii) The duration of x rays is controlled by that of laser. The x-ray power bursts in a very sharp and short pulse (comparable to the laser pulse length). On the other hand, in the blackbody x rays, the duration time becomes much longer because it is decided by atomic processes. Irradiating such x rays on certain atoms with appropriate conditions should lead to ultrafast inner-shell excitation.

II. ATOMIC PROCESSES

Illustrated in Fig. 1 are schematic atomic processes along with the associated x-ray emission by inner-shell ionized atoms. The upper (lower) states of laser correspond to $2p^5 3s (2p^6)$, $2p^5 3s^2 (2p^6 3s)$, and $2p^5 3s^2 3p (2p^6 3s 3p)$; and the wavelengths are 40, 25, and 17 nm for Na, Mg, Al atoms, respectively. Since the calculated gain length products agree well with those measured in their experiments for Cd vapor in Ref. [7], we adopt a similar atomic process model. Namely, we consider only fast atomic processes, that is, photoionization, autoionization, electron-impact ionization, and radiative transition. The photoionization and electron-impact ionization cross sections (σ^P and σ^e) are derived from the data or empirical formulas in Refs. [17,18] and [19,20], respectively. The energy levels, radiative transition probabilities, and autoionization rates are calculated with the use of Cowan's code [21,22].

The rates of change of concentrations of the various atomic states as illustrated in Fig. 1 may be governed by the following equations:

$$\dot{N}_0 = -(R_{0,1} + R_{0,2}) N_0,$$
$$\dot{N}_1 = R_{0,1} N_0 - D_1 N_1, \quad (2)$$
$$\dot{N}_2 = R_{0,2} N_0 + D_2 N_2,$$

with $R_{i,j} = R^e_{i,j} + R^P_{i,j}$. The subscripts 0, 1, 2 correspond to the initial atom, upper states (inner-shell excited states), and lower states, respectively. The coefficient D_i expresses the decay rate for state i, that is, $D_1 = A_a + A_r + R_{1,3}$ and $D_2 = R_{2,4}$. The rates R^P, R^e, A_r, and A_a are those of photoionization, electron-impact ionization, radiative transition probability, and autoionization, respectively. Here R^P and R^e are given by

$$R^P = \int_{E_{\mathrm{lion}}}^{\infty} \frac{I\sigma^P}{h\nu_I} d(h\nu_I), \quad (3)$$

$$R^e = \int_{E_{\mathrm{eion}}}^{\infty} v_e \sigma^e n_e dE_e, \quad (4)$$

respectively, where E_e, n_e, I, and $h\nu_I$ are the electron-impact energy, population of the electrons, intensity of the source (driving) x rays, and photon energy. The ionization energies E_{eion} and E_{lion} are those for photoionization and electron-impact ionization, respectively. For the analysis of the x-ray laser, the gain Γ of soft x rays from the lasing process by the transition between an upper state and a lower state is given by

$$\Gamma = 2.7 \times 10^{-2} \phi_i \frac{P}{g} f_{\mathrm{ul}},$$

with

$$P = N_{\mathrm{up}} - g N_{\mathrm{low}}, \quad g = g_{\mathrm{low}}/g_{\mathrm{up}}, \quad (5)$$

where $N_{\mathrm{up(low)}}$, $g_{\mathrm{up(low)}}$, and f_{ul} are the population, statistical weight of the upper (lower) state, and oscillator strength, and ϕ_i is the lifetime of the upper state.

III. X-RAY LASER CONDITIONS

The populations $N_0 - N_2$ in Eq. (2) may be analytically solved as follows [6]:

$$N_0 = N_{00} e^{-(R_{0,1}+R_{0,2})t}, \quad N_1 = \frac{R_{0,1} N_{00}}{R^{0,1} - D_1} (e^{-D_1 t} - e^{-(R_{0,1}+R_{0,2})^t}),$$

$$N_2 = \langle v_e \sigma^e_{0,2} \rangle R_{01} N_{00}^2 \left[\frac{1}{R_{0,1}-D_1} \left(\frac{1}{D_2 - D_1 - R_{0,1}} e^{-(D_1+R_{0,1})t} - \frac{1}{D_2 - 2R_{0,1}} e^{-2R_{0,1}t} \right) + \frac{1}{(D_2 - 2R_{0,1})(D_2 - D_1 - R_{0,1})} e^{-D_2 t} \right], \tag{6}$$

where N_{00} is the density of the vapor and n_e can be the population of electrons ejected mainly from the target through the inner-shell photoionization process. Therefore, we can set

$$n_e \sim \sum_i N_i \sim N_1. \tag{7}$$

The N_i values can be expanded in terms of low-order processes because of the short duration time. Then the populations of the upper (N_1) and lower (N_2) states can be obtained as [5]

$$N_1 \sim R_{0,1} N_{00} \{ t - (R_{0,1} + D_1) t^2/2 \}, \tag{8}$$

$$N_2 \sim \langle v_e \sigma^e_{0,2} \rangle R_{0,1} N_{00}^2 t^2/2. \tag{9}$$

Here in the Na, Mg, and Al vapor, D_2 is so small that it is ignored. The population inversion P in Eq. (5) becomes as follows:

$$P = R_{0,1} N_{00} [t - (R_{0,1} + D_1 + g \langle v_e \sigma^e_{0,2} \rangle N_{00}) t^2/2], \tag{10}$$

where only fast processes such as $R^P_{0,1}$, $R^P_{1,3}$, and $g\langle v_e \sigma^e_{0,2} \rangle$ are considered. The maximum value $P_{\max}$ of population inversion and duration time ($t_{\rm dur}$) of x-ray laser are given by

$$P_{\max} = \frac{R_{0,1} N_{00}}{2(R_{0,1} + D_1 + g \langle v_e \sigma^e_{0,2} \rangle / N_{00})}, \tag{11}$$

$$t_{\rm dur} = 2 \{ R_{0,1} + D_1 + g \langle v_e \sigma^e_{0,2} \rangle N_{00} \}^{-1}. \tag{12}$$

We find that the duration time in a vapor target is much longer than that in a solid target. For example, $t_{\rm dur} = 100$ fs, 0.1 fs for vapor (10^{19} cm^3) and solid (10^{22} cm^3) for the typical values of $v_e = 10^8$ cm/s, $\sigma^e_{0,2} \sim 10^{-15}$ cm^2 and $g = 10$. The maximum gain $\Gamma_{\max}$ in Eq. (5) can be rewritten by

$$\Gamma_{\max} \sim 2.7 \times 10^{-2} \frac{1}{D_1} \frac{R_{0,1} N_{00}}{2g(R_{0,1} + D_1 + g \langle v_e \sigma^e_{0,2} \rangle N_{00})} f_{\rm ul}$$

$$\sim 2.7 \times 10^{-2} \frac{1}{D_1} \times \frac{I \sigma^P_{0,1} N_{00}}{2g(I \sigma^P_{0,1} + D_1 + g \langle v_e \sigma^e_{0,2} \rangle N_{00} h\nu_I)} f_{\rm ul}. \tag{13}$$

We see that in the case of $D_1 \sim g \langle v_e \sigma^e_{0,2} \rangle N_{00}$, the $\Gamma_{\max}$ is saturated. Then the initial density ($N_{00,\rm sat}$) is obtained as

$$N_{00,\rm sat} = \frac{D_1}{g \langle v_e \sigma^e_{0,2} \rangle}. \tag{14}$$

With the use of previous values for D_1, g, v_e, and $\sigma^e_{0,1}$, $N_{00,\rm sat} = 10^{18}$ cm^{-3}. Further, the Γ of ~ 10 cm^{-1} may be obtained in the case of $\sigma^P_{0,1} = 10^{-18}$ cm^2, $h\nu_I = 100$ eV, and $I = 10^{12}$ W/cm^2.

IV. THE TARGET AND DRIVER

We explore target materials and x-ray pumping sources in order to find an optimized class of inner-shell ionization x-ray laser. We show that the Na, Mg, and Al vapor target and Larmor x rays are suitable for this laser.

A. Target material

The Auger rates for the L-shell inner-shell excited states of vapor of Mg and Al ($\sim 10^{12}$ s^{-1}) are much smaller than those of K-shell inner-shell excited states ($> 10^{14}$ s^{-1}) [11]. (In the Na, Auger decay does not occur.) As seen from Eq. (5), the longer lifetime of the inner-shell excited states is related to higher gain. Further, the lower density is expected to produce a longer duration time [3,4,6].

Figure 2 shows the gain as a function of time for Na, Mg, and Al vapor at 10^{19}-cm^{-3} density. We consider the x-ray intensity of 10^{12} W/cm^2 with 0–500-eV photoenergy. A 10 cm^{-1} gain at 100 fs is expected for these vapors. In our previous paper [6] the x-ray intensities of 10^{15} W/cm^2 and 10^{13} W/cm^2 are required for the creation of hollow atoms and for the inner-shell ionization x-ray laser method of NaH solid, respectively. The inner-shell ionization method of NaH solid is precarious, as the duration time is shorter than 1 fs. On the other hand, the current inner-shell ionization x-ray laser method with these vapors is far more realistic because of the long duration time and high gain.

Figure 3 shows the x-ray intensity dependence for gain on a Mg vapor target with 10^{19}-cm^{-3} density. For $I \leqslant 10^{13}$ W/cm^2, the gain increases, as the x-ray intensity becomes larger. The gain duration time (~ 100 fs) is about the same over a wide range of the pump power. On the other hand, for higher intensities $I \geqslant 10^{13}$ W/cm^2, a different behavior is found. The maximum gain remains about the same for different I and the duration time decreases according to I^{-1}. This is in agreement with Eqs. (11), (12), and (13). For a low x-ray intensity ($D_1 \ll g \langle v_e \sigma^e_{0,2} \rangle N_{00}$), $P_{\max}$ and $t_{\rm dur}$ may be rewritten as

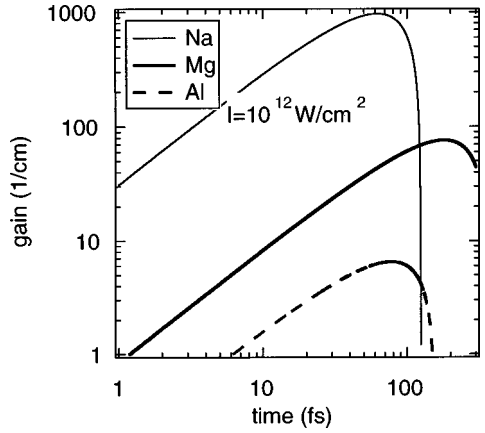

FIG. 2. Gain (1/cm) vs time (fs) for inner-shell ionization x-ray laser of Na, Mg, and Al vapor with 10^{19}-cm^{-3} density. The pumping x-ray source has the intensity of 10^{12} W/cm^2 and constant photoenergy distribution.

$$P_{\max}=\frac{R_{0,1}}{g\langle v_e\sigma^e_{0,2}\rangle}\propto I,N^0_{00}, \tag{15}$$

and

$$t_{\rm dur}=2\{g\langle v_e\sigma^e_{0,2}\rangle N_{00}\}^{-1}\propto I^0,N^{-1}_{00}. \tag{16}$$

Namely, $P_{\max}$ ($t_{\rm dur}$) is (inversely) proportional to $I(N_{00})$ and remains constant for various $N_{00}(I)$. On the other hand, for $D_1\gg g\langle v_e\sigma^e_{0,2}\rangle N_{00}$, we have

$$P_{\max}=\frac{R_{0,1}N_{00}}{2(R_{0,1}+D_1)}\propto I^0,N_{00} \tag{17}$$

and

$$t_{\rm dur}=2\{R_{0,1}+D_1\}^{-1}\propto I^{-1},N^0_{00}. \tag{18}$$

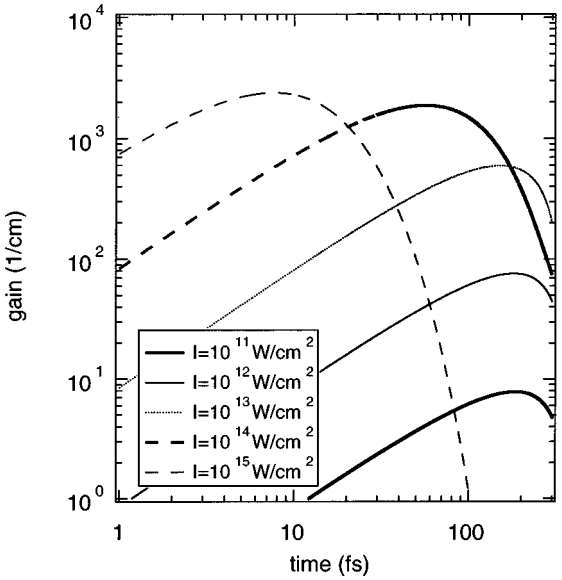

FIG. 3. Gain (1/cm) vs time (fs) for inner-shell ionization x-ray laser of Mg vapor with 10^{19}-cm^{-3} density and various intensity of x-ray source.

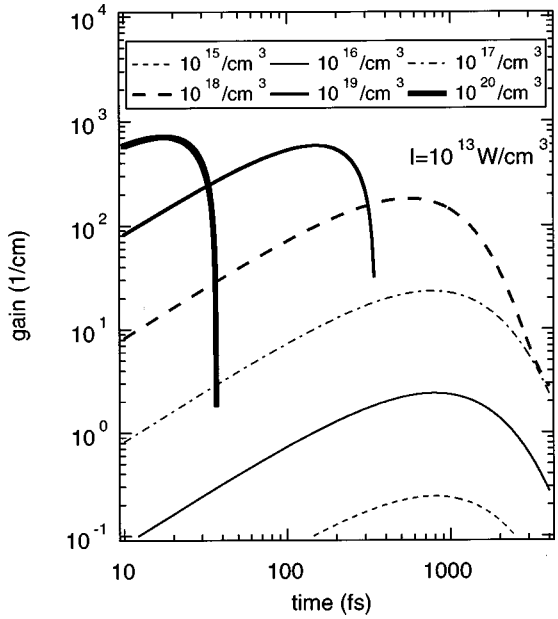

FIG. 4. Gain (1/cm) vs time (fs) for inner-shell ionization x-ray laser of Mg vapor with $I=10^{13}$ W/cm^2 and various vapor density.

In this case, $P_{\max}$ ($t_{\rm dur}$) increases (decreases) according to $N_{00}(I^{-1})$ and is the same value for different $I(N_{00})$. As the autoionization and radiative transition are independent of the intensity of x rays, only the multi-inner-shell ionization dominates in high brightness x rays [6].

Figure 4 shows the gain Γ as a function of time at $I=10^{13}$ W/cm^2 for various densities of Mg vapor. At low density, the gain increases in proportion to the density and the duration time remains constant ($\sim$1 ps) for various N_{00}. Equations (17) and (18) indicate these scalings. In this case, the gain and duration time are determined by the x-ray intensity and the lifetime of upper states, respectively. While for high density ($N_{00}\geqslant 10^{18}$ cm^{-3}), the duration time decreases as the density becomes greater and $P_{\max}$ remains constant for various N_{00}, as shown in Eqs. (15) and (16). The short duration time results from the secondary electron impact ionization, which destroys the inversion population as shown in Refs. [2–4, 6].

B. X-ray source

In Ref. [6] Larmor x rays are employed as a pump x-ray source for producing the inner-shell excited states of atoms. Larmor x rays can have high brightness and short pulse as mentioned before. As the large population of the upper states (inner-shell excited states) is required in order to obtain high gain, high brightness x rays are useful to overcome the loss of population due to fast autoionization and electron-impact ionization. By the short pulse, the intensity of x rays can be weakened after a large population of inner-shell excited states is obtained. The high-intensity x rays play a role of disturbance for atomic structure. Since the Larmor x rays have an energy peak, we can achieve high conversion efficiency from incoherent x rays to fluorescent x rays by setting the peak energy just above the inner-shell ionization threshold energy where the ionization cross sections are the largest.

Figure 5 shows the same as Fig. 2 for a Larmor x-ray pump source at $E_{\rm pk}=100$ eV ($a_0\sim 5$). The gain is about

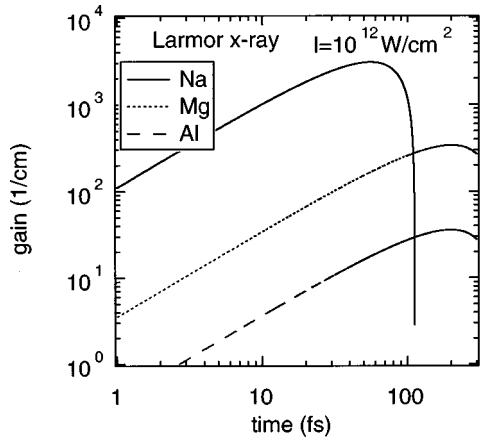

FIG. 5. Gain (1/cm) vs time (fs) for inner-shell ionization x-ray laser of Na, Mg, and Al vapor with 10^{19}-cm^{-3} density pumped by Larmor x-ray source with $E_{pk}=100$ eV.

three times as large as that in Fig. 2, though the duration time is the same. In bremsstrahlung x rays, since the flat photoenergy distribution is in the range of 0–1000 keV at $a_0=5$, the gain is much smaller than that in Fig. 2.

Figure 6 shows the gain vs time for various x-ray intensity I given by Eq. (1). We treat the electron density n_e as a constant and we employ the scaling equation:

$$I=I_{(100\ \mathrm{eV})}(10^{-2}E_{pk})^{2/3}, \tag{19}$$

because of $E_{pk}\propto a_0^3$ and $I\propto a_0^2$ where the x-ray spectrum peaks at E_{pk} and the yielded x-ray intensity is I and $I_{100\,\mathrm{eV}}=10^{12}$ W/cm^2. The gain decreases as E_{pk} (or a_0) increases. The duration time does not vary much except for the case of $E_{pk}\sim 80$ eV. For $E_{pk}\sim 80$ eV, the energy spectrum of free electrons is mostly lower than the threshold energy and the secondary electron-impact ionization becomes slower. We should adjust a_0 in such a way to make E_{pk} just above the inner-shell ionization threshold energy ($\sim$80 eV). Then we can achieve higher conversion efficiency for x-ray laser. However, we have a large enough gain even at $E_{pk}=200$ eV.

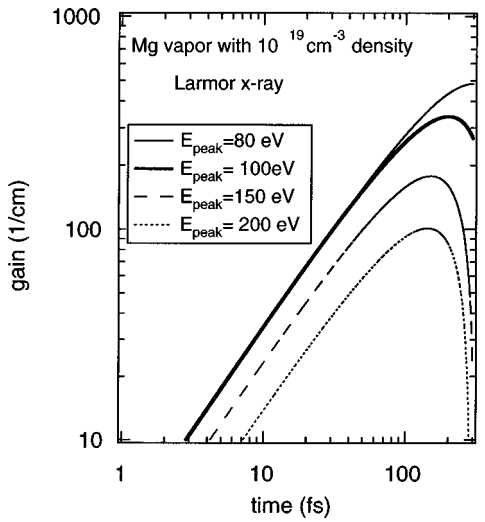

FIG. 6. Gain (1/cm) vs time (fs) for inner-shell ionization x-ray laser of Mg vapor with 10^{19}-cm^{-3} density and Larmor x-ray source with various E_{pk} values.

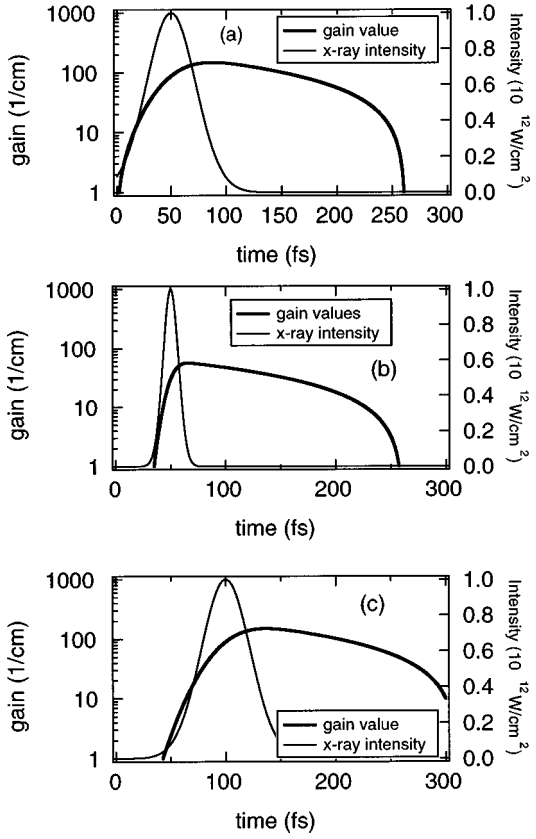

FIG. 7. Gain (1/cm) vs time (fs) for inner-shell ionization x-ray laser of Mg vapor of 10^{19}-cm^{-3} density and time-dependent Larmor x-ray source with $E_{pk}=100$ eV.

Figure 7 shows the gain Γ with the use of a time-dependent x-ray pump source for Mg vapor. The time-dependent intensity of the source may be given by

$$I(t)=I_0\exp[-a(t-t_{pk})^2] \tag{20}$$

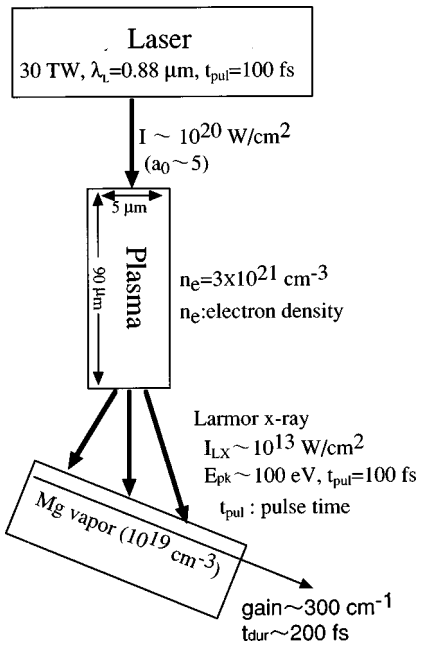

FIG. 8. An example of detailed requirements for the experiment.

with $I_0=10^{12}\,\mathrm{W/cm^2}$, $N_{00}=10^{19}\,\mathrm{cm^{-3}}$, $t_{\mathrm{pk}}=50$ or 100 fs. The gain in Fig. 7(b) is about half as large as that in Figs. 7(a) and 7(c). However, the time dependence of the source does not change the result by much.

Figure 8 shows an example of detailed requirements for an experiment. As soon as the high-intensity ($10^{20}\,\mathrm{W/cm^2}$, $a_0\sim 5$) short-pulse (100 fs) laser irradiates the plasma with $n_e=3\times 10^{21}\,\mathrm{cm^{-3}}$, $R_s=5\,\mu\mathrm{m}$, and $R_L=90\,\mu\mathrm{m}$, the high brightness ($10^{13}\,\mathrm{W/cm^2}$) short-pulse (100 fs) Larmor x rays with $E_{\mathrm{pk}}=100\,\mathrm{eV}$ are emitted. By using the Larmor x rays for an x-ray pump source and Mg vapor with 10^{19}-$\mathrm{cm^{-3}}$ density for a target, the inner-shell ionization x-ray laser with large Γ ($\sim 300\ \mathrm{cm^{-1}}$) may be realized.

V. SUMMARY

We have optimized an inner-shell ionization x-ray laser with the use of a high-intensity short-pulse Larmor x-ray pump source and the adoption of vapor of Na, Mg, and Al as a target material. Such vapor makes the inner-shell ionization process dominant. A high gain x-ray lasing ($>10\ \mathrm{cm^{-1}}$) may be obtained with an x-ray source of $10^{12}\,\mathrm{W/cm^2}$. We have also studied the gain as a function of the vapor density and x-ray intensity. The different trends are expected for the saturated and unsaturated regimes of the density and intensity. In the unsaturated regime, the gain increases in proportion to the density and intensity. After the saturation occurs, the gain remains constant for various densities and x-ray intensities. On the other hand, the duration decreases, as the densities and intensities increase. Since the Larmor x rays have high brightness and short pulse, it is suitable for the inner-shell ionization. The high brightness is important for an ultrafast inner-shell ionization. The short pulse plays an important role in keeping the atomic structure intact. A Larmor x-ray spectrum has an energy peak as a function of the laser intensity of $E_{\mathrm{pk}}\propto a_0^3$. The high conversion efficiency may be achieved by setting the peak energy just above the inner-shell ionization threshold energy where the ionization cross sections are the largest.

ACKNOWLEDGMENTS

We wish to thank Dr. Y. Ueshima, Dr. H. Ihara, Dr. S. Goto, Dr. K. Kawanishi, Dr. K. Nagashima, Dr. Y. Kato, Dr. H. Takuma, Dr. T. Arisawa, and Dr. K. Shinohara, for their useful discussions. R. D. Cowan's code is employed for the atomic structures. T.T. is supported in part by the NSF and U.S. DOE.

[1] M. A. Duguay and M. Rentzepis, Appl. Phys. Lett. **10**, 350 (1967).
[2] T. S. Axelrod, Phys. Rev. A **13**, 376 (1976).
[3] H. C. Kapteyn, Appl. Opt. **31**, 4391 (1992).
[4] S. J. Moon, D. C. Eder, and G. L. Strobel, in *X-ray Lasers*, Proceedings of the Fourth International Colloquium, Williamburg, VA, 1994, edited by David C. Eder and Dennis L. Matthews AIP Conf. Proc. No. **332** (AIP, New York, 1994).
[5] G. L. Strobet, D. C. Eder, and P. Amendt, Appl. Phys. B: Lasers Opt. **B58**, 45 (1994).
[6] K. Moribayashi, A. Sasaki, and T. Tajima, Phys. Rev. A **58**, 2007 (1998).
[7] W. T. Silfvast, J. J. Macklin, and O. R. Wood II, Opt. Lett. **8**, 551 (1983).
[8] H. C. Kapteyn, R. W. Lee, and R. W. Falcone, Phys. Rev. Lett. **57**, 2939 (1986).
[9] H. C. Kapteyn and R. W. Falcone, Phys. Rev. A **37**, 2033 (1988).
[10] S. Meyer, T. Menzel, B. Wellegehausen, P.-X. Lu, S. Insam, and E. Fill, in *X-ray Lasers 1996*, edited by S. Svanberg and C. G. Wahlström, IOP Conf. Proc. No. 151 (Institute of Physics and Physical Society, London, 1996), p. 173.
[11] O. K. Rahkonen and M. O. Krause, At. Data Nucl. Data Tables **14**, 139 (1974).
[12] Y. Kinjo, K. Shinohara, A. Ito, H. Nakano, M. Watanabe, Y. Horiike, Y. Kikuchi, M. C. Richardson, and K. A. Tanaka, J. Microsc. **176**, 63 (1994).
[13] L. D. Landua and E. M. Lifshifz, *Classical Field Theory* (Pergamon Press, New York, 1992), Sec. 48, p. 110 and Sec. 73, p. 194.
[14] P. Gibbon, Phys. Rev. Lett. **76**, 50 (1996).
[15] Y. Ueshima, Y. Kishimoto, A. Sasaki, Y. Sentoku, and T. Tajima, in *Proceedings of the First JAERI-Kansai International Workshop on Ultrashort-Pulse Ultrahigh-Power Lasers and Simulation for Laser-Plasma Interactions, Kyoto, Japan, 1997*, edited by Kansai Research Establishment (JAERI, Tokai, 1997), Vol. 98-004, p. 31.
[16] Y. Ueshima, Y. Kishimoto, A. Sasaki, and T. Tajima, Laser Part Beams (to be published).
[17] J. J. Yeh and I. Lindau, At. Data Nucl. Data Tables **32**, 1 (1985).
[18] Y. B. Zel'dovich and Y. P. Raizer, *Physics of Shock Waves and High Temperature Hydrodynamic Phenomena* (Academic Press, New York, 1966), p. 265.
[19] W. Lotz, Z. Phys. **232**, 101 (1970).
[20] L. B. Golden and D. H. Sampson, J. Phys. B **10**, 2229 (1977).
[21] R. D. Cowan, J. Opt. Soc. Am. **58**, 808 (1968).
[22] R. D. Cowan, *The Theory of Atomic Structure and Spectra* (University of California, Press, Berkeley, 1981).